# Modelling of Ethanol Fermentation Coupled with Product Recovery by Pervaporation

# BOGDAN TRICA, OANA CRISTINA PARVULESCU\*, TANASE DOBRE, ALI A.A. AL JANABI, CRISTIAN RADUCANU, CLAUDIA PATRICHI

Politehnica University of Bucharest, Chemical and Biochemical Engineering Department, 1-3 Gheorghe Polizu Str., 011061, Bucharest, Romania

Bioethanol is the most important biofuel produced by fermentation of sugars from various biomass types. The main disadvantages associated to this process consist in the negative effect of high ethanol concentration on the cell growth and in the separation cost of ethanol-water system resulted in the fermentation process. Sugar fermentation using Saccharomyces cerevisiae yeast coupled with bioethanol recovery by pervaporation has been modeled and simulated in this paper. In order to avoid the clogging of pervaporation membrane, the yeast cells were previously retained into an ultrafiltration unit. Three operating modes were analyzed and compared, i.e., classical batch fermentation (BF), batch fermentation coupled with external ultrafiltration and pervaporation (BFPV). Surface areas of ultrafiltration and pervaporation units were selected as process control variables.

Keywords: ethanol fermentation, fed batch bioreactor, modelling, pervaporation, solvent recovery, ultrafiltration

Biofuels derived from renewable resources are realistic and perhaps one day will become economic substitutes to fossil fuels. Bioethanol produced by biomass fermentation is widely used in the sectors of energy and materials [1-7]. During the traditional ethanol batch fermentation process, the accumulation of ethanol in the biosynthesis mass inhibits cell growth leading to low ethanol concentration in the fermentation broth, causing a lot of energy consumed for its recovery [8]. Currently, bioethanol synthesis is developed following three major research directions. The first one refers to finding new technologies capable of exploiting as many vegetal resources containing fermentable sugars as possible. The second direction is related to the adaptation or development of new microbial systems with enhanced tolerance to high concentrations of ethanol in the fermentation broth. The third one refers to bioethanol separation which should lead to a minimization of production costs. Modern separation technologies based on the removal of ethanol from the fermentation broth by gas stripping, extraction, adsorption, distillation, and pervaporation have been developed. Ethanol removal by gas stripping occurs by its transfer into a gas stream. This procedure, which uses carbon dioxide produced in the fermentation process as a gaseous stripping media, was conceptually appealing owing to its simplicity and ability to operate at the same temperature as that of the fermentation reactor, thus without lethal action to the cells [9-11]. Ethanol fermentation coupled with product extraction involves the mass transfer of the ethanol from the fermentation broth to a suitable extractant [8,12-14]. By using a coupled adsorption/fermentation process, ethanol is preferentially transferred to a solid adsorbent material, which is insoluble in the broth and has a high selectivity for ethanol [15-18]. Pervaporation is one of the most promising approaches for the recovery of alcohols or other solvents from fermentation broths [19-22]. Referring to the effect of fermentation by-products on the purification of ethanol from water using pervaporation, it was proved that sugars and salts increased the membrane

performance, whereas butanediol and glycerol (secondary ethanoic fermentation products) decreased the ethanol flux and selectivity of pervaporation membrane [19].

This paper aims at modelling and simulating sugar fermentation using *Saccharomyces cerevisiae* yeast coupled with bioethanol recovery by pervaporation. In order to avoid clogging of the pervaporation surface, an ultrafiltration unit was inserted between the fermenter and the pervaporation unit, its retentate being recycled into the fermenter.

# Modelling of ethanol fermentation coupled with product pervaporation

Total flux and membrane selectivity for pervaporation of ethanol dilute solutions

Various membrane types have been studied in the pervaporation recovery of organic compounds from watercontaining streams. Due to their hydrophobic and organophilic properties, rubbery polymers have been recognized as potential materials for pervaporation applications. Polydimethylsiloxane (PDMS) is the most common silicone rubber material used in these applications. The separation factor ( $\alpha$ ) of PDMS membranes used for ethanol-water pervaporation commonly ranges from 4 to 20 [22-24]. Characteristic total flux (J.) of this membrane type is relatively low, i.e., cca. 1  $kg/(m^2 \times h)$  [25,26]. The modification of PDMS membranes with special fillers such as hydrophobic zeolites, referring specifically to rubber based composite membranes, has also been studied [26,27]. In many cases, the ethanolwater separation factor of these modified membranes has been increased (up to 55), whereas the total flux has been generally kept at a value of about 1 kg/( $m^2 \times h$ ). In the past decades, inorganic zeolite membranes [28-30] have also been extensively studied for pervaporation applications. Zeolite membranes are claimed to offer some advantages over polymeric membranes, e.g., they do not swell, are

more stable chemically than polymeric ones, can tolerate high temperatures resulting in high permeate fluxes.

Zeolite membranes with separation action in a microfilm (MFI), especially silicalite type membranes, have been widely studied for removing organics from water-containing streams. The advantage of silicalite type membranes in the separation of ethanol from aqueous solutions is attributed to the hydrophobic properties and well-defined pore size of silicalite crystals [31]. Ethanol-water separation factors over 106 have been reported for some pervaporation MFI membranes, while the total flux was slightly over 1 kg/(m²×h). The aim in zeolite membrane synthesis is to produce membranes that are as thin as possible. Zeolite membranes are typically synthesized onto porous inorganic supports, which are needed to ensure the mechanical strength of the thin membranes

To design membranes for specific applications and predict their performances, a deep understanding of transport phenomena is required. However, it is challenging to develop a mass transfer model for pervaporation applicable for all types of membrane materials and separated mixtures. The swelling behaviour of polymeric membranes and the multi-feature diffusion mechanisms through inorganic membranes prohibit the development of a universal mass transfer model for pervaporation [31,32].

A silicalite membrane synthesized onto a ceramic tube was considered in this paper. If the ethanol fermentation of sugar species (glucose) produces only ethanol, the permeate concentrations in ethanol ( $c_E$ ) and glucose ( $c_S$ ) as well as the process temperature (t) can be considered as process factors affecting the membrane total flux ( $J_t$ ) and separation factor ( $\alpha$ ). Tables 1 and 2 contain data adapted from the related literature [31,33-35]) and organized according to a  $2^3$  factorial plan. Minimal, central (0), and maximal (max) levels of process factors are specified in table 1, where coded values of process factors were given by eqs. (1)-(3). Values of process performances in terms of  $J_t$  and  $\alpha$  for various levels of coded factors ( $X_t$ ,  $X_s$ , and  $X_s$ ) are summarized in table 2.

$$X_1 = \frac{c_E - c_{E0}}{c_{E,\text{max}} - c_{E0}} = \frac{c_E - 80}{60} \tag{1}$$

$$X_2 = \frac{c_S - c_{S0}}{c_{S,\text{max}} - c_{S0}} = \frac{c_S - 120}{100}$$
 (2)

$$X_3 = \frac{t - t_0}{t_{\text{max}} - t_0} = \frac{t - 50}{20} \tag{3}$$

Regression equations showing the dependence of  $J_{\nu}$  (eq. (4)) and  $\alpha$  (eq. (5)) on the process factors were obtained by processing the data presented in table 2 according to the characteristic procedure of a  $2^3$  factorial plan [36-38]. These equations along with the species balances for the pervaporation device represent the basic mathematical model of the pervaporation unit. This model coupled with that of a fermentation bioreactor can accurately describe the integrated processes.

$$J_{\rm r}(X_1, X_2, X_3) = 0.681 + 0.249X_1 + 0.286X_3 + 0.114X_1X_3$$
 (4)

$$\alpha(X_1, X_2, X_3) = 47.88 + 13.375X_1 \tag{5}$$

Modelling of the ethanol fermentation

Ethanol is industrially produced in batch, continuous, fed batch or semi-continuous systems. In batch fermentation, the substrate and yeast culture are charged into the

Table 1
LEVELS OF PROCESS FACTORS FOR PV DEHYDRATION OF ETHANOL USING A MFI SILICALITE MEMBRANE

	Nat	Coded factors				
Level	$\frac{c_E}{(\text{kg/m}^3)}$	cs (kg/m <sup>3</sup> )	<i>t</i> (°C)	$X_1$	<i>X</i> <sub>2</sub>	<i>X</i> <sub>3</sub>
Minima1	20	20	30	-1	-1	-1
Central	80	120	50	0	0	0
Maximal	140	220	70	+1	+1	+1

 Table 2

 EXPERIMENTATION MATRIX FOR PV DEHYDRATION OF ETHANOL

No.	Xı	<i>X</i> <sub>2</sub>	<i>X</i> <sub>3</sub>	$J_t$ (kg/(m <sup>2</sup> ×h))	α
1	+1	+1	+1	1.23	59
2	+1	+1	-1	0.58	57
3	+1	-1	+1	1.43	65
4	+1	-1	-1	0.48	64
5	-1	+1	+1	0.59	35
6	-1	+1	-1	0.23	34
7	-1	-1	+1	0.62	39
8	-1	-1	-1	0.29	38

bioreactor along with the nutrients. The main advantages of batch systems are their easy control and great flexibility.

In the continuous process, the feed containing substrate, culture medium, and other required nutrients is continuously pumped into an agitated vessel which contains active microorganisms. The product, which is taken from the bottom of the bioreactor, contains ethanol, cells, and residual sugar. Fermentation systems operated in a continuous mode offer several advantages compared to batch processes, generally resulting in enhanced volumetric productivity and, consequently, smaller bioreactor volumes and lower investment and operational costs. The major drawback is that the yeasts cultivated under anaerobic conditions over a long period have a diminished ability to synthesize ethanol. Moreover, at high dilution rates enabling elevated productivities, the substrate is not completely consumed and ethanol yields are reduced [39].

In fed batch operation, the feed solution, which contains the substrate, yeast culture, and required minerals and vitamins, is fed at constant intervals, while effluent is discontinuously removed. The main advantage of the fed batch system is that the intermittent feeding of the substrate prevents inhibition. If the substrate has an inhibitory effect, intermittent addition improves the productivity of the fermentation by maintaining a low substrate concentration.

In semi-continuous processes, a portion of the culture is withdrawn at intervals and fresh medium is added to the system. This method has some of the advantages of continuous and batch operations. There is no need for a separate inoculum vessel, except at the initial start-up. Another advantage is that not much control is required. However, there is a high risk of contamination and mutation due to long cultivation periods and periodic handling.

Despite their drawbacks, bioreactors operated in batch or fed batch mode are widely used in current industrial practice. Mathematical models describing batch and fed batch fermentations are mainly based on characteristic equations of process kinetics and mass balance.

#### Fermentation kinetics

Various kinetic models have been developed for the growth of *S. cerevisiae* yeast cells in batch or continuous

glucose fermentation. Among them, unstructured models provide a good understanding of the global metabolism of microbiological processes [40-42]. These unstructured models fairly approximate the dynamics of ethanol fermentation processes, especially for batch or fed batch operation. Cellular growth rate,  $v_{p\chi}$  (kg/(m³×h)), can be determined by Monod equation (6), where  $c_s$  (kg/m³) is the concentration of the limiting substrate,  $c_\chi$  (kg/m³) the concentration of yeast cells,  $\mu_{max}$  (h¹) the maximum specific growth rate of microorganims, and  $K_s$  (kg/m³) the substrate saturation constant.

$$v_{RX} = \mu_{\max} \frac{c_{S}}{K_{S} + c_{S}} c_{X}$$
 (6)

This equation describes well the fermentation processes as the growth of the fermenting organism is not inhibited by toxic substances. For glucose fermentation with S. cerevisiae it can be used only for low glucose concentrations. Microbial activity during ethanol fermentation is affected by certain factors, including cell death, substrate limitation, substrate inhibition, and product inhibition. The influence of all these factors on the S. cerevisiae cellular growth rate is expressed by eq. (7) [43,44], where  $K_L$  (m³/kg) is the substrate inhibition parameter,  $K_d$  (h¹) the constant of cellular death rate,  $c_{X_{max}}$  (kg/m³) and  $c_{E_{max}}$  (kg/m³) are the yeast and ethanol concentrations  $E_{max}$  which the growth ceases,  $E_{max}$  and  $E_{max}$  are empirical parameters.

The ethanol production rate  $(v_{pp})$  is given by eq. (8), where  $Y_{EX}$  (kg/kg) is the product yield based on cell growth and  $\beta_E$  (h<sup>-1</sup>) a parameter related to the ethanol biosynthesis by yeast cells. The substrate consumption rate  $(v_{pq})$  is expressed by eq. (9), where  $Y_X$  (kg/kg) is the limit cellular yield and  $\beta_S$  (h<sup>-1</sup>) a parameter similar to  $\beta_E$ . According to the data reported in the related literature for a culture medium based on sucrose or glucose at a concentration level of 50-250 g/L and a fermentation temperature of 2040

Table 3TEMPERATURE DEPENDENCE/VALUES OF PARAMETERS<br/>CHARACTERIZING GLUCOSE FERMENTATIONWITH S. CEREVISIAE FOR t=20-40 °C AND  $c_c=50-250$  g/L

 $^{\circ}$ C [43,45-48], characteristic parameters of eqs. (7)-(9) are summarized in table 3.

$$v_{RX} = \mu_{\max} \frac{c_S}{K_S + c_S} c_X \left( \exp(K_i c_S) \right) \left( 1 - \frac{c_X}{c_{X \max}} \right)^n \left( 1 - \frac{c_E}{c_{E \max}} \right)^n - K_d c_X$$
(7)

$$v_{RE} = Y_{EX}v_{RX} + \beta_E c_X \tag{8}$$

$$v_{RS} = v_{RX} / Y_X + \beta_S c_X \tag{9}$$

Physical model of ethanol fermentation coupled with product pervaporation

The physical model describing ethanol biosynthesis coupled with product pervaporation is shown in figure 1. The pervaporation device is protected from clogging with cellular material by an ultrafiltration device mounted between the bioreactor and the pervaporation unit.

The process of ethanol fermentation coupled with product recovery occurred as follows: (i) a broth stream from the bioreactor (1) was fed by a pump (2) into the ultrafiltration device (3), where the yeast cells were kept in the retentate; (ii) the ultrafiltration retentate was recycled into the bioreactor and the ultrafiltration permeate was fed by a pump (4) into the pervaporation device (5); (iii) the pervaporation retentate was recycled into the bioreactor, whereas the permeate vapour was condensed in a heat exchanger (6) and further fed into a collector (7).

Three operating modes were considered, *i.e.*, batch fermentation (BF), batch fermentation coupled with ultrafiltration and pervaporation (BFPV), and fed batch fermentation coupled with ultrafiltration and pervaporation (FBFPV). FBFPV involves the following procedure: (i) start BF; (ii) switch BF to fed batch fermentation (FBF) by feeding a concentrated substrate ( $\tau_{Pl} = 5$  min); (iii) start the ultrafiltration and pervaporation processes ( $\tau_{Pl} = 10$  min); (iv) switch FBF to BF ( $\tau_{Pl} = 45$  min). BFPV operating mode includes only steps (i) and (iii).

The parameters in figure 1 are as follows: V and  $V_c$  are the volumes of liquid phase in the bioreactor and in the

No.	Parameter	Equation	Units	No.	Parameter	Value	Units
1	$\mu_{\max}$	0.26(t/20)-0.075	h-l	7	$K_S$	4.23	kg/m <sup>3</sup>
2	C Emax	260-106(t/20)	$kg/m^3$	8	$K_i$	0.002	m <sup>3</sup> /kg
3	C Xmax	269-120(t/20)	$kg/m^3$	9	$\beta_E$	0.095	h-l
4	$Y_{EX}$	10.6(t/20)-10.25	kg/kg	10	βs	0.19	h-l
5	$Y_X$	0.19-0.08(t/20)	kg/kg	11	m	1	-
6	$K_d$	0.54-0.12(t/20)	h-l	12	n	1.5	-

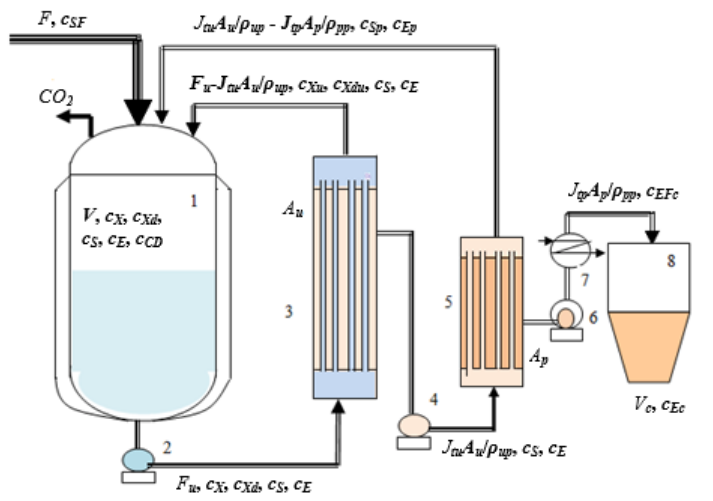


Fig. 1. Scheme of ethanol fermentation coupled with ultrafiltration and volatile species pervaporation:
(1) bioreactor, (2) ultrafiltration pump, (3) ultrafiltration device, (4) pervaporation pump, (5) pervaporation device, (6) vacuum pump, (7) condenser, (8) collector of condensed pervaporation permeate.

collector of condensed pervaporation permeate,  $c_{S}$ ,  $c_{E}$ ,  $c_{X}$ ,  $c_{XD}$  and  $c_{CD}$  the concentrations of substrate (sugar), ethanol, viable S. cerevisiae cells, dead S. cerevisiae cells, and carbon dioxide in the bioreactor, F and  $F_{u}$  the feed flow rates of bioreactor and ultrafiltration device,  $c_{Xu}$  and  $c_{Xdu}$  the concentrations of active and dead cells in the ultrafiltration retentate,  $c_{SF}$  and  $c_{Sp}$  the concentrations of substrate in the bioreactor feed and in the pervaporation retentate,  $c_{Ep}$ ,  $c_{EFC}$ , and  $c_{Ec}$  the concentrations of ethanol in the pervaporation retentate, in the feed of collector of condensed pervaporation permeate, and in the collector,  $J_{uu}$  and  $J_{tp}$  the total fluxes of ultrafiltration and pervaporation permeates,  $\rho_{up}$  and  $\rho_{pp}$  the densities of ultrafiltration and (condensed) pervaporation permeates,  $A_{u}$  and  $A_{p}$  the surface areas of ultrafiltration and pervaporation membranes.

## Mass balance in the bioreactor

Total and partial mass balances in the bioreactor are expressed by eqs. (10)-(15), whereas  $c_{\it EFC}$   $c_{\it EL}$ ,  $c_{\it Sp}$ ,  $c_{\it Xu'}$  and  $c_{\it Xdu}$  parameters in eqs. (10)-(15) are given by eqs. (16)-(20), where  $m_{\it CD}$  (kg) is the mass of carbon dioxide,  $M_{\it CD}$ ,  $M_{\it E}$ ,  $M_{\it up}$ , and  $M_{\it pp}$  (kg/kmole) are the molar masses of carbon

$$\frac{dV}{d\tau} = F - \frac{J_{tp}A_p}{\rho_{pp}} \tag{10}$$

$$\frac{d(Vc_{Xd})}{d\tau} = VK_dc_X - F_uc_{Xd} + (F_u - J_{tu}A_u / \rho_{up})c_{Xdu}$$
(11)

$$\frac{d(Vc_X)}{d\tau} = Vv_{RX} - F_u c_X + (F_u - J_{tu} A_u / \rho_{up}) c_{Xu}$$
(12)

$$\frac{d(Vc_S)}{d\tau} = -Vv_{RS} + Fc_{SF} - J_{tu}A_uc_S / \rho_{pu} + (J_{tu}A_u / \rho_{up} - J_{tp}A_p / \rho_{pp})c_{Sp}$$
 volume of liquid phase collected in the tank a m<sup>3</sup>) the ethanol concentration in the collector.

$$\frac{d(Vc_{E})}{d\tau} = Vv_{RE} - J_{tu}A_{u}c_{E} / \rho_{up} + (J_{tu}A_{u} / \rho_{up} - J_{tp}A_{p} / \rho_{pp})c_{Ep}$$
(14)

$$\frac{dm_{CD}}{d\tau} = \frac{M_{CD}}{M_E} \left[ V v_{RE} - J_{tx} A_u c_E / \rho_{up} + (J_{tx} A_u / \rho_{up} - J_{tp} A_p / \rho_{pp}) c_{Ep} \right]$$
(15)

$$c_{EFc} = \frac{\alpha(c_E)c_E \frac{M_{wp}\rho_{pp}}{M_{pp}\rho_{wp}}}{1 + [\alpha(c_E) - 1]c_E \frac{M_{wp}}{M_E\rho_{wp}}}$$

$$(16)$$

$$c_{Ep} = \frac{J_{tu}A_{u}c_{E} - J_{tp}A_{p}c_{EFc}}{J_{tu}A_{u} - J_{tp}A_{p}}$$
(17)

$$c_{Sp} = \frac{J_{tu}A_{u}c_{S}}{J_{tu}A_{u} - J_{tv}A_{v}}$$
 (18)

$$c_{Xu} = \frac{F_u c_X}{F_u - J_{tu} A_u / \rho_{up}}$$
 (19)

$$c_{Xdu} = \frac{F_{u}c_{Xd}}{F_{v} - J_{v}A_{v} / \rho_{vv}}$$
 (20)

dioxide, ethanol, ultrafiltration permeate, and condensed pervaporation permeate.

Total ultrafiltration permeate flux

Some assumptions regarding the ultrafiltration device were made: (i) ethanol biosynthesis was neglected due to the short residence time of ultrafiltration retentate; (ii) ultrafiltration permeate did not contain any S. cerevisiae cells; (iii) substrate and ethanol concentrations were the same in the ultrafiltration retentate and permeate, i.e.,  $c_s$  and  $c_r$ .

Total ultrafiltration permeate flux,  $J_{tu}(kg/((m^2 \times h)))$ , was determined by eq. (21), where  $\eta(kg/(m \times s))$  is the permeate viscosity,  $R_0(m^{-1})$  the initial membrane resistance,  $r_g(kg/(m^3 \times s))$  the gel layer specific resistance,  $\Delta p(N/m^2)$  the transmembrane pressure,  $c_\chi(kg/m^3)$  the biomass concentration in the bioreactor,  $c_{\chi_g}(kg/m^3)$  the biomass concentration in the gel layer, and  $\tau(h)$  the time [49].

$$J_{tu} = 3600 \left( \frac{1}{(\eta R_0)^2 + 3600} \frac{1}{\frac{2r_g \Delta p c_X}{c_{Xg}}} \tau \right)^{0.5} \Delta p$$
 (21)

For an ultrafiltration unit based on a tubular ceramic membrane and for superficial velocities of retentate inside the tube over 2 m/s, the following values of parameters in eq. (21) were reported [49-52]:  $R_0 = 2-1210^{13} \ \mathrm{m}^{-1}$  and  $r_g/c_{\chi g} = 3-8^{109} \ \mathrm{s}^{-1}$ .

Mass balance in the collector of condensed pervaporation permeate

The collecting tank of condensed pervaporation permeate was assumed as a perfectly mixed vessel characterized by eqs. (22) and (23), where  $V_c$  (m³) is the volume of liquid phase collected in the tank and  $c_{Ec}$  (kg/m³) the ethanol concentration in the collector.

$$\frac{dV_c}{d\tau} = \frac{J_{tp}A_p}{\rho_{xx}} \tag{22}$$

$$\frac{dc_{Ec}}{d\tau} = \frac{J_{tp}A_p(c_{EFc} - c_{Ec})}{\rho_{pp}V_c}$$
(23)

Mathematical model of ethanol fermentation coupled with product pervaporation

Mathematical model describing the coupled processes is based on 8 differential equations, *i.e.*, eqs. (10)-(15), (22), and (23), which determine the dynamics of V,  $C_x$ ,  $C_{x,c}$ ,  $C_x$ ,  $C_x$ ,  $C_y$ ,  $C_z$ , and  $C_z$ . Ethanol batch fermentation (BF), ethanol batch fermentation coupled with ethanol recovery by pervaporation (BFPV), and ethanol fed batch fermentation coupled with ethanol recovery by pervaporation (FBFPV) were simulated depending on the parameters specified in table 4 and those determined by eqs. (1)-(5), (7)-(9), and (16)-(21).

## **Results and discussions**

Dynamics of broth volume, concentrations of sugar, ethanol, active and dead cells, as well as carbon dioxide mass in the bioreactor are shown in figs. 2-4. Results on the dynamics of total permeate flux for ultrafiltration and pervaporation processes, liquid volume in the collector of pervaporation permeate, mean ethanol concentration in the collector, ethanol concentrations in the permeate and

Table 4INPUT PARAMETERS FOR BF, BFPV, AND FBFPV

3.7	7		DEDI	EDEDI:
No.	Process factors	BF	BFPV	FBFPV
1	Initial broth volume in the bioreactor, V <sub>0</sub> (m <sup>3</sup> )	50	50	20
2	Initial sugar concentration in the bioreactor, cs (kg/m <sup>3</sup> )	150	150	150
3	Initial active cells concentration in the bioreactor, $c_{X0}$ (kg/m <sup>3</sup> )	1.5	1.5	1.5
4	Initial dead cells concentration in the bioreactor, cxa0 (kg/m³)	0.15	0.15	0.15
5	Initial volume of liquid phase in the collector of pervaporation permeate, $V_{c0}$ (m <sup>3</sup> )	-	0.01	0.01
6	Initial ethanol concentration in the collector, cEc0 (kg/m <sup>3</sup> )	-	0.1	0.1
7	Processing time, ty(h)	100	100	100
8	Surface area of ultrafiltration device, $A_{II}$ (m <sup>2</sup> )	-	470, 300	470, 300
9	Surface area of pervaporation device, $A_p$ (m <sup>2</sup> )	-	340, 170	340, 170
10	Pervaporation start time, \(\tau_{PV}(h)\)	-	10	10
11	Fed batch start time, τ <sub>F1</sub> (h)	-	-	5
12	Fed batch stop time, τ <sub>F2</sub> (h)	-	-	45
13	Bioreactor feed flow rate, F (m <sup>3</sup> /h)	-	-	1.2
14	Sugar concentration in the reactor feed, csf (kg/m <sup>3</sup> )	-	-	250
15	Ultrafiltration device feed flow rate, $F_u$ (m <sup>3</sup> /h)	-	20	20
16	Net ultrafiltration pressure difference, $\Delta p$ (bar)	-	1	1
17	Pervaporation permeate pressure (mbar)	-	70	70
18	Bioreactor temperature (°C)	30	30	30
19	Pervaporation device temperature (°C)	60	60	60

retentate of pervaporation unit are presented in figures 5-7. Data depicted in figures 2-7 reveal the following issues:

(i) the broth volume (V) for BFPV (curves 2 and 3 in fig. 2a) decreased almost linearly, indicating an almost constant total permeate flux of pervaporation device (according to the data presented in figure 6b, where the values of  $J_p$  are close to a mean value of 0.6 kg/( $m^2$ ´h) (curve 2) and 0.5 kg/( $m^2$ ´h) (curve 3), respectively); the broth volume for FBFPV (curves 4 and 5 in fig. 2a) increased from  $\tau_{Pl} = 5$  h to  $\tau_{P2} = 45$  h (between start and stop time of fed batch operation) because the feed flow rate was larger than that of pervaporation permeate;

(ii) no major differences are observed in terms of sugar consumption rates for BF and BFPV (curves 1-3 in fig. 2b); the operation time of 31 h found for BF is also close to those of BFPV, *i.e.*, 29 h (curve 2 in fig. 2b) and 28 h (curve

3 in fig. 2b); sugar concentration ( $c_s$ ) for FBFPV (curves 4 and 5 in fig. 2b) decreased in the first 5 h from 150 g/L to 136 g/L, because is no feed, then it increased in the next 7 h, and further decreased due to an increase in the fermentation rate;

(iii) dynamics of concentrations of active and dead cells (fig. 3) were similar for BF, BFPV, and FBFPV; for  $c_s$ <15 g/L, the concentration of active cells ( $c_x$ ) decreased linearly with the time (fig. 3a), whereas that of dead cells ( $c_{xd}$ ) increased linearly (fig. 3b);

(iv) dynamics of ethanol concentration inside the bioreactor ( $c_E$ ), presented in figure 4a, reveal an increase up to a value of 71 g/L (which was reached at about 30 h) followed by a constant plateau for BF (curve 1); for BFPV (curves 2 and 3) and FBFPV (curves 4 and 5), ethanol concentration exhibited the same trend as that of active

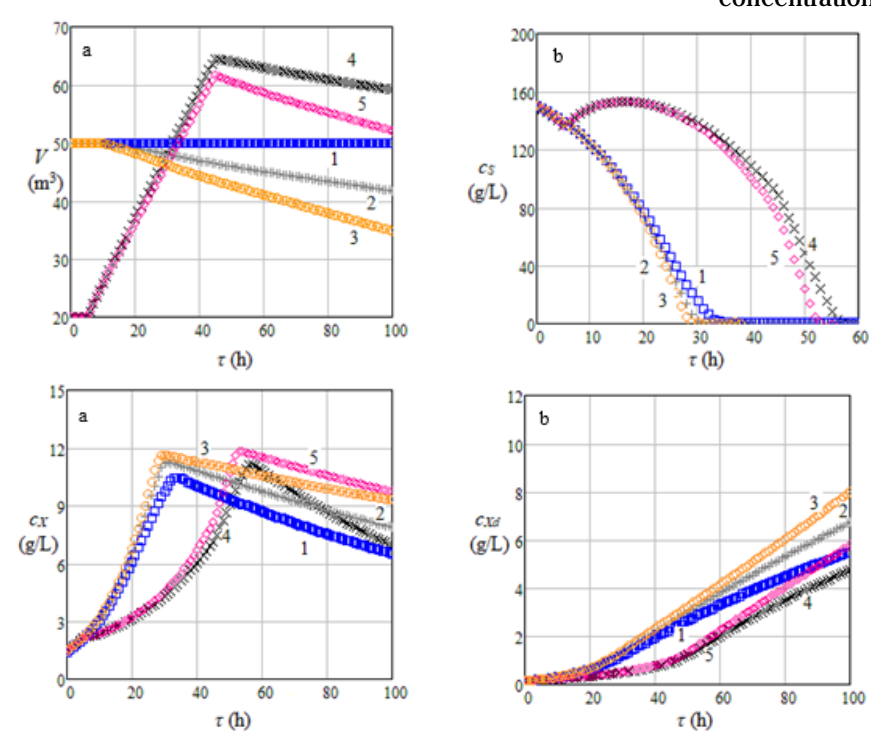


Fig. 2. Dynamics of broth volume (**a**) and sugar concentration (**b**) in the bioreactor: (1) BF; (2) BFPV ( $A_u$ =300 m²,  $A_p$ =170 m²,  $F_u$ =20 m³/h); (3) BFPV ( $A_u$ =470 m²,  $A_p$ =340 m²,  $F_u$ =20 m³/h); (4) FBFPV ( $A_u$ =300 m²,  $A_p$ =170 m²,  $F_u$ =20 m³/h); (5) FBFPV ( $A_u$ =470 m²,  $A_p$ =340 m²,  $F_u$ =20 m³/h)

Fig. 3. Concentration dynamics of active cells (a) and dead cells (b) in the bioreactor: (1) BF; (2) BFPV ( $A_u$ =300 m²,  $A_p$ =170 m²,  $F_u$ =20 m³/h); (3) BFPV ( $A_u$ =470 m²,  $A_p$ =340 m²,  $F_u$ =20 m³/h); (4) FBFPV ( $A_u$ =300 m²,  $A_p$ =170 m²,  $F_u$ =20 m³/h); (5) FBFPV ( $A_u$ =470 m²,  $A_p$ =340 m²,  $F_u$ =20 m³/h).

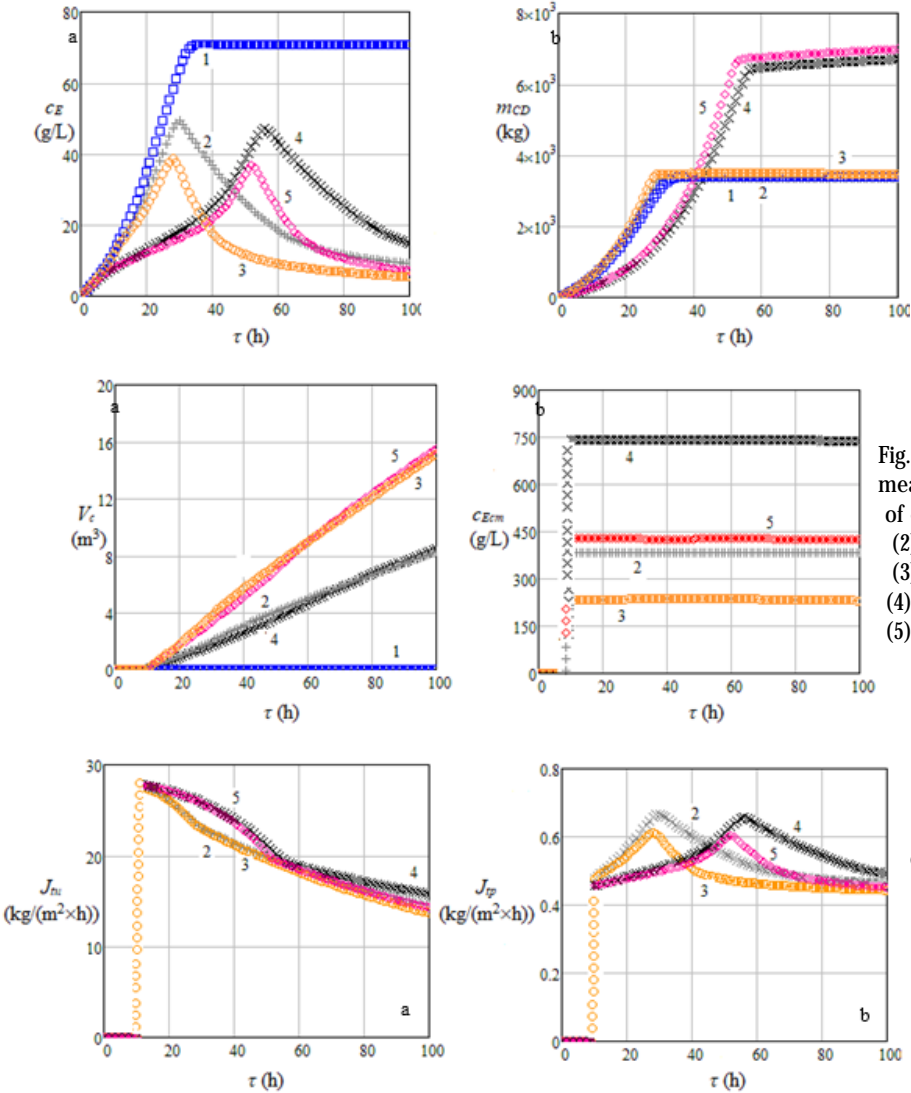


Fig. 4. Dynamics of ethanol concentration (a) and carbon dioxide mass (b) in the bioreactor: (1) BF; (2) BFPV  $(A_n = 300 \text{ m}^2, A_n = 170 \text{ m}^2,$  $F_{\nu} = 20 \text{ m}^3/\text{h}$ ; (3) BFPV ( $A_{\nu} = 470 \text{ m}^2$ ,  $A_{\nu} = 340$  $m^2$ ,  $F_n = 20 \text{ m}^3/\text{h}$ ; (4) FBFPV  $(A_n = 300 \text{ m}^2, A_n = 170 \text{ m}^2, F_n = 20 \text{ m}^2)$  $m^3/h$ ); (5) FBFPV ( $A_n = 470 \text{ m}^2$ ,  $A_n = 340 \text{ m}^2$ ,

 $F_{\rm u}=20\,{\rm m}^3/{\rm h}$ ).

Fig. 5. Dynamics of liquid phase volume (a) and mean ethanol concentration (b) in the collector of condensed pervaporation permeate: (1) BF; (2) BFPV  $(A_n = 300 \text{ m}^2, A_n = 170 \text{ m}^2, F_n = 20 \text{ m}^3/\text{h});$ 

- (3) BFPV ( $A_n = 470 \text{ m}^2$ ,  $A_n = 340 \text{ m}^2$ ,  $F_n = 20 \text{ m}^3/\text{h}$ );
- (4) FBFPV ( $\tilde{A}_{\mu}$ =300 m<sup>2</sup>,  $\tilde{A}_{\mu}$ =170 m<sup>2</sup>,  $\tilde{F}_{\mu}$ =20 m<sup>3</sup>/h);
- (5) FBFPV ( $A_n^2 = 470 \text{ m}^2$ ,  $A_n^2 = 340 \text{ m}^2$ ,  $F_n^2 = 20 \text{ m}^3/\text{h}$ ).

Fig. 6. Dynamics of total permeate flux of ultrafiltration (a) and pervaporation (b) devices: (1) BF; (2) BFPV  $(A_{1}=300 \text{ m}^{2}, A_{2}=170 \text{ m}^{2})$  $m^2$ ,  $F_n = 20 \text{ m}^3/\text{h}$ ; (3) BFPV ( $A_n = 470 \text{ m}^2$ ,  $A_n = 340 \text{ m}^2$ ,  $F_n = 20 \text{ m}^3/\text{h}$ ; (4) FBFPV ( $A_n = 300 \text{ m}^3/\text{h}$ );  $m^2$ ,  $A_p = 170 \text{ m}^2$ ,  $F_u = 20 \text{ m}^3/\text{h}$ ; (5) FBFPV  $(A_u = 470 \text{ m}^2, A_b = 340 \text{ m}^2, F_u = 20 \text{ m}^3/\text{h}).$ 

cells, i.e., it increased up to 40-50 g/L (at about 30 h for BFPV and 50 h for FBFPV) and then decreased, the maximum values of  $c_E$  being higher for lower level of surface areas of ultrafiltration and pervaporation

membranes ( $A_u$ =300 m² and  $A_z$ =170 m²); (v) the mass of carbon dioxide produced during the fermentation process  $(m_{CD})$  was almost double for FBFPV (curves 4 and 5 in fig. 4b) than for BF and BFPV (curves 1-3 in fig. 4b) as an effect of substrate feed between  $\tau_{_{Pl}}$ =5 h and  $\tau_{_{Pl}}$ =45 h; (vi) liquid phase volume in the collector of condensed

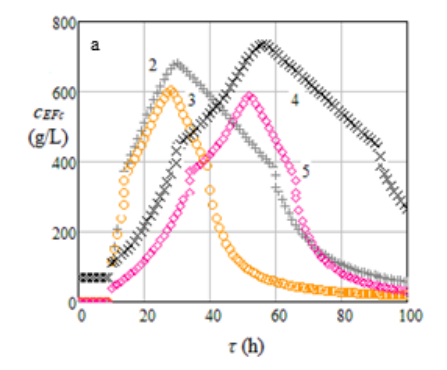
pervaporation permeate  $(V_c)$  increased nearly linearly over time for BFPV (curves 2 and 3 fig. 5a) and FBFPV (curves 4 and 5 fig. 5a), indicating an almost constant total permeate flux of pervaporation device  $(J_{tp})$ , as shown in fig. 6b; mean ethanol concentration in the collector  $(c_{Ecm})$ , which is presented in fig. 5b, was higher for FBFPV (up to

773 g/L) than for BFPV (up to 383 g/L); moreover, higher

levels of  $A_u$  and  $A_v$  resulted in higher values of  $V_c$  and lower values of  $c_{E_{CM}}$ , respectively.

(vii) total permeate flux of ultrafiltration device  $(J_{uu})$  decreased over time for BFPV (curves 2 and 3 in fig. 6a) and FBFPV (curves 4 and 5 in fig. 6a) and it is higher for FBFPV; dynamics of total permeate flux of pervaporation device  $(J_m)$ , which are shown in fig. 6b, as well as of ethanol concentrations in the condensed permeate  $(c_{\rm \tiny EEC})$  and retentate  $(c_{ED})$  of pervaporation (fig. 7) exhibit the same trend as those of ethanol concentration in the bioreactor (fig. 4a).

Some advantages of coupled processes are revealed by results summarized in table 5. The major advantage consists in obtaining a pervaporation product having a high mean ethanol concentration (up to 773 kg/m<sup>3</sup> for FBFPV and up to 383 kg/m<sup>3</sup> for BFPV). The ethanol can be used as



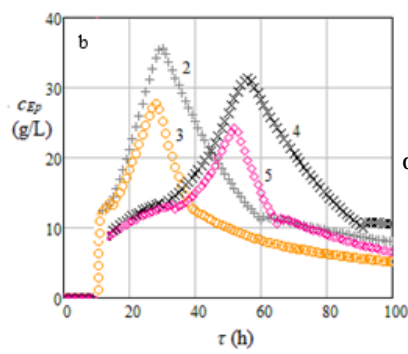


Fig. 7. Dynamics of ethanol concentrations in the permeate (a) and retentate (b) of pervaporation device: (1) BF; (2) BFPV ( $A_u$ =300 m²,  $A_p$ =170 m²,  $F_u$ =20 m³/h); (3) BFPV ( $A_u$ =470 m²,  $A_p$ =340 m²,  $F_u$ =20 m³/h); (4) FBFPV  $(A_n = 300 \text{ m}^2, A_n = 170 \text{ m}^2, F_n = 20 \text{ m}^3/\text{h});$  (5) FBFPV ( $A_{u}^{"}=470 \text{ m}^{2}, A_{p}^{"}=340 \text{ m}^{2}, F_{u}^{"}=20 \text{ m}^{3}/\text{h}$ )

**Table 5**MAIN RESULTS FOR BF, BFPV, AND FBFPV

No.	Operating mode	BF	BFPV	BFPV	FBFPV	FBFPV
1	Surface area ratio, Au/Ap	-	300/170	470/340	300/170	470/340
2	Initial broth volume in the bioreactor, V0 (m3)	50	50	50	20	20
3	Initial sugar concentration in the bioreactor, con (kg/m3)	150	150	150	150	150
4	Sugar concentration in the reactor feed, csf (kg/m3)	-	-	-	250	250
5	Processing time, tf(h)	100	100	100	100	100
6	Final ethanol concentration in the bioreactor, cg/(kg/m <sup>3</sup> )	70.86	9.13	5.41	14.39	5.69
7	Final sugar concentration in the bioreactor, csr (kg/m3)	0.623	0.28	0.092	0.12	0.07
8	Mean ethanol concentration in the collector of condensed pervaporation permeate, $c_{Ecm}$ (kg/m <sup>3</sup> )	-	383	231	773.2	423
9	Processed sugar mass (kg)	7469	7488	7503	14990	15010
10	Produced ethanol mass (kg)	3583	3514	3656	7070	7080
11	Produced carbon dioxide mass (kg)	3484	3467	3499	6860	6890
12	Active cells mass at the end of the process (kg)	257.9	269.3	274.1	329.7	432.7
13	Died cells mass at the end of the process (kg)	264.3	272.6	270.6	268.6	289.6
14	Sugar conversion to ethanol (kg/kg)	0.461	0.459	0.465	0.461	0.461
15	Water mass to be evaporated for producing 1 kg of absolute ethanol (kg/kg)	9.98	1.41	3.11	0.276	1.213

such or concentrated by pervaporation to absolute ethanol. The water mass to be evaporated for producing 1 kg of absolute ethanol was as follows: 0.276 kg/kg (A/A=300/170) and 1.213 (A/A=470/340) for FBFPV, 1.41 kg/kg (A/A=300/170) and 3.11 kg/kg (A/A=470/340) for BFPV, and 9.98 kg/kg for BF, respectively. Moreover, at the end of processing time (100 h), the sugar concentration in the bioreactor was lower for FBFPV (up to 0.12 kg/m³) than for BFPV (up to 0.28 kg/m³) and BF (0.623 kg/m³), whereas the sugar conversion to ethanol was almost invariant, *i.e.*, 0.459-0.465 kg/kg, irrespective of operating mode. The main disadvantages of the BFPV and FBFPV operating modes are the high surface area values of ultrafiltration and pervaporation units and the clogging of ultrafiltration surface.

### **Conclusions**

A process of ethanol fermentation of glucose from molasses sugars or starch hydrolysates coupled with ethanol pervaporation has been analyzed. Classical batch fermentation (BF), batch fermentation with external ultrafiltration and pervaporation (BFPV), and fed batch fermentation with external ultrafiltration and pervaporation (FBFPV) were compared. The computation steps considered for modelling of these operating modes were as follows: (i) selection of the membrane type for the ultrafiltration and pervaporation devices; (ii) modelling of the ultrafiltration device in order to express the transmembrane flux; (iii) modelling of the pervaporation device for determining the permeate flux and separation factor depending on the liquid composition and pervaporation temperature; (iv) selection of the fermentation kinetics; (v) establishment of characteristic equations of each operating mode. The main advantage of coupled processes consisted in controlling the inhibition of fermentation process and in obtaining a pervaporation product with a high ethanol concentration (up to 773 kg/ m<sup>3</sup> for FBFPV and up to 383 kg/m<sup>3</sup> for BFPV for a processing time of 100 h), whereas the major disadvantages of BFPV and FBFPV were the high surface area of ultrafiltration and pervaporation devices and the clogging of ultrafiltration surface.

Acknowledgements: Ali A. A. Al Janabi expresses his gratitude to the Iraqi Ministry of Higher Education and Scientific Research as well as to the Al-Furat Al-Awsat Technical University for their funding.

### References

- 1. AVRAM, M., STROESCU, M., STOICA-GUZUN, A., FLOAREA, O., DOBRE, T., Rev. Chim. (Bucharest), **66**, no. 1, 2015, p. 79.
- 2. BAEYENS, J., KANG, Q., APPELS, L., DEWIL, R., LV, Y., TAN, T., Prog. Energy Combust. Sci, 47, 2015, p. 60.
- 3. BALAT, M., BALAT, H., Appl. Energy, 86, 2009, p. 2273.
- 4. BRUNSCHWIGA, C., MOUSSAVOUA, W., BLIN, J., Prog. Energy Combust. Sci. 38, no. 2, 2012, p. 283.
- 5. CALINESCU, I., CHIPURICI, P., ALEXANDRESCU, E., TRIFAN, A., Cent. Eur. J. Chem., 12, no. 8, 2014, p. 851.
- 6. CALINESCU, I., CHIPURICI, P., TRIFAN, A., BADOIU, C., UPB Sci. Bull., Series B, **74**, no. 1, 2012, p. 33.
- 7. GHITA, D., STANICA-EZEANU, D., CURSARU, D., ROSCA, P., Rev. Chim. (Bucharest), **67**, no. 1, 2016, p. 145.
- 8. LARSSON, M., ZACCHI, G., Bioprocess Biosyst. Eng., 15, no. 3, 1996, p. 125.
- 9. DOMINGUEZ, J.M., CAO, N., GONG, C.S., TSAO, G.T., Biotechnol. Bioeng., **67**, 2000, p. 336.
- 10. TAYLOR, F., KURANTZ, M.J., GOLDBERG N., CRAIG JR., J.C., Biotechnol. Lett., **20**, 1998, p. 67.
- 11. TAYLOR, F., KURANTZ, M.J., GOLDBERG, N., MCALOON, A.J., CRAIG, J., Biotechnol. Prog., **16**, 2000, p. 541.
- 12. BOTHUN, G.D., KNUTSON, B.L., STROBEL, H.J., NOKES, S.E., BRIGNOLE, E.A., DIAZ, S., J. Supercrit. Fluid, **25**, 2003, p. 119.
- BOUDREAU, T.M., HILL, G.A., Process Biochem., 41, 2006, p. 980.
   GYAMERAH, M., GLOVER, J., J. Chem. Technol. Biotechnol., 66, 1996, p. 145.
- 15. BOWEN, T.C., VANE, L.M., Langmuir, 22, 2006, p. 3721.
- 16. CARTON, A., BENITO, G.G., REY, J.A., FUENTE, M.D.L., Bioresour. Technol., **66**, 1998, p. 75.
- 17. HOLTZAPPLE, M.T., BROWN, R.F., Sep. Technol., **4**, 1994, p. 213. 18. OUMI, Y., MIYAJIMA, A., MIYAMOTO, J., SANO, T., Stud. Surf. Sci. Catal., **142**, 2002, p. 1595.
- 19. CHOVAU, S., GAYKAWAD, S., STRAATHOF, A.J., VAN DER BRUGGEN,

- B., Bioresour. Technol., 102, 2011, p. 1669.
- 20. DONG, Z., GONGPING, L., SAINAN, L., ZHENGKUN, L., WANQIN, J., J. Membr. Sci., **450**, 2014, p. 38.
- 21. LEE, H.J., CHO, E.J., KIM, Y.G., CHOI, I.S., BAE, H.J., Bioresour. Technol., **109**, 2012, p. 110.
- 22. CHEN, X., PING, Z., LONG, Y., J. Appl. Polym. Sci., **67**, no. 4, 1998, p. 629.
- 23. ROZICKA, A., NIEMISTO, J., KEISKI, R.L., KUJAWSKI, W., J. Membr. Sci., **453**, 2014, p. 108.
- 24. VANE, L.M., J. Chem. Technol. Biotechnol., 80, 2005, p. 603.
- 25. SHIRAZI, Y., GHADIMI, A., MOHAMMADI, T., J. Appl. Polym. Sci., **124**, no. 4, 2012, p. 2871.
- 26. VANE, L.M., NAMBOODIRI, V.V., BOWEN, T.C., J. Membr. Sci., **308**, no. 1–2, 2008, p. 230.
- 27. PENG, P., SHI, B., LAN, Y., Sep. Sci. Technol., 46, no. 3, 2011, p. 420
- 28. LIN, X., CHEN, X., KITA, H., OKAMOTO, K., AICHE J., **49**, no. 1, 2003, p. 237.
- 29. LIN, X., KITA, H., OKAMOTO, K., Ind. Eng. Chem. Res., **40**, no. 19, 2001, p. 4069.
- 30. MORIGAMI, Y., KONDO, M., ABE, J., KITA, H., OKAMOTO, K., Sep. Purif. Technol., **25**, no. 1–3, 2001, p. 251.
- 31. LEPAJARVI, T., MALINEN, I., KORELSKIY, D., KANGAS, J., DEDLUND, J., TANSKAANEN, J., Period. Polytech. Chem., **59**, no. 2, 2015, p. 11. 32. AL JANABI, A.A.A., PARVULESCU, O.C., DOBRE, T., ION, V.A., Rev. Chim. (Bucharest), **67**, no. 1, 2016, p. 150.
- 33. CHEN, H., Li, Y., YANG, W., J. Membr. Sci., 296, 2007, p. 122.
- 34. LEPAJARVI, T., Pervaporation of alcohol/water mixtures using ultrathin zeolite membranes, Ph.D. Thesis, University of Oulu, 2015. SANO, J., YANAGISHITA, H., KIYOZUMI, Y., MIZAKAMI, F., HARAYA, K., J. Membr. Sci., **95**, 1994, p. 221.
- 36. CIOROIU, D.R., PARVULESCU, O.C., KONCSAG, C.I., DOBRE, T., RADUCANU, C., Rev. Chim. (Bucharest), **68**, no. 10, 2017, p. 2311.

- 37. ORBECI, C., PARVULESCU, O.C., ACCELEANU, E., DOBRE, T., Rev. Chim. (Bucharest), **68**, no. 10, 2017, p. 2325.
- 38. PARVULESCU, O.C., GAVRILA, A.I., DÖBRE, T., CEATRA, L., Rev. Chim. (Bucharest), **67**, no. 11, 2016, p. 2254.
- 39. SANCHEZ, O., CARDONA, C.A., Bioresour. Technol., **99**, 2008, p. 5270
- 40. RAMON-PORTUGAL, F., DELIA-DUPUY, M.L., PINGAUD, H., RIBA, J.P., J. Chem. Technol. Biotechnol., **68**, no. 2, 1997, p. 195.
- 41. TAN, Y., WANG, Z.X., MARSHALL, K.C., Biotehnol. Bioeng., **52,** no. 5, 1996, p. 602.
- 42. WARREN, R.K., HILL, G.A., MACDONALD, D.G., Biotechnol. Prog., 6, no. 5, 1990, p. 319.
- 43. RIVERA, C.E., COSTA, C.A., ATALA, I.P.D., MAUGERI, F., MACIEL, R.W.M., MACIEL, F.R., Process Biochem., 41, 2006, p. 1682.
- 44. RIVERA, C.E., YAMAKAWA, K.C., GARCIA, H.M., GERALDO, C.V., ROSSELL, E.V.C., MACIEL, F.R., BONOMIA, A., Chem. Eng. Trans., 32, 2013, p. 1369.
- 45. ANDRADE, R.R., RIVERA, E.C., ATALA, D.I.P., MACIEL, F.R., MAUGERI, F.F., COSTA, A.C., Bioprocess Biosyst. Eng., **32**, 2009, p. 673.
- 46. ATALA, D.I.P., COSTA, A.C., MACIEL, F.R., MAUGERI, F., Appl. Biochem. Biotechnol., **91–93**, 2001, p. 353.
- 47. HOLZBERG, I., FINN, R.K., STEINKRAUS, K.H., Biotechnol. Bioeng., **9**, no. 3, 1967, p. 413.
- 48. HOPPE, G., HANSFORD, G., Biotechnol. Lett., **41**, 1982, p. 39. 49. AL JANABI, A.A.A., DOBRE, T., PARVULESCU, O.C., DANCIU, T.D., PATRICHI, C., Rev. Chim. (Bucharest), **66**, no. 12, 2015, p. 2070.
- 50. BAE, T.H., TAK, T.M., J. Membr. Sci., **264**, no. 1, 2005, p. 151.
- 51. KABSCH-KORBUTOWICZ, M., URBANOWSKA, A., Environ. Prot. Eng., **36**, no. 1, 2010, p. 125.
- 52. VINCENT-VELA, M.C., CUARTAS-URIBE, B., ALVAREZ-BLANCO, S., LORA-GARCIA, J., Desalination **284**, 2012, p. 14.

Manuscript received: 3.08.2016